Research Article | Vol. 25, No. 7 | 3 Apr 2017 | OPTICS EXPRESS 7627

Optics EXPRESS

Broad expansion of optical frequency combs by self-Raman scattering in coupled-cavity self-mode-locked monolithic lasers

M. T. CHANG,[1] T. L. HUANG,[1] H. C. LIANG,[2] K. W. SU,[1] AND Y. F. CHEN[1,*]

[1]*Department of Electrophysics, National Chiao Tung University, 1001 Ta-Hsueh Rd. Hsinchu 300, Taiwan*

[2]*Institute of Optoelectronic Science, National Taiwan Ocean University, Keelung 20224, Taiwan*

**yfchen@cc.nctu.edu.tw*

Abstract: Broad expansion of optical frequency comb (OFC) by the self-Raman scattering is numerically analyzed and experimentally accomplished in a coupled-cavity self-mode-locked (SML) monolithic Yb:KGW laser. The gain medium is coated to achieve the monolithic SML operation and a partially reflective mirror is further exploited to form the coupled cavity and to multiply the repetition rate up to 128.9 GHz. With a coupled reflectivity of 95%, it is experimentally found that not only the first-order but also second-order stimulated Raman scattering (SRS) can be efficiently generated. The mode-locked OFC can be consequently expanded to reach approximately 8.4 THz, leading the pulse width to be as narrow as 53 fs. At the pump power of 8.7 W, the total output power for the fundamental and the first- and second-Stokes waves can be maintained at 1.6 W. The present exploration provides a promising way to generate the ultrahigh-repetition-rate broadband OFC via the simultaneous SML and SRS processes.

OCIS codes: (140.3580) Lasers, solid-state; (140.3480) Lasers, diode-pumped; (140.4050) Mode-locked lasers; (140.3550) Lasers, Raman; (140.3615) Lasers, ytterbium.

References and links

1. V. Gerginov, C. E. Tanner, S. A. Diddams, A. Bartels, and L. Hollberg, "High-resolution spectroscopy with a femtosecond laser frequency comb," Opt. Lett. **30**(13), 1734–1736 (2005).
2. S. T. Cundiff and J. Ye, "Colloquium: Femtosecond optical frequency combs," Rev. Mod. Phys. **75**(1), 325–342 (2003).
3. T. Udem, R. Holzwarth, and T. W. Hänsch, "Optical frequency metrology," Nature **416**(6877), 233–237 (2002).
4. S. T. Cundiff and A. M. Weiner, "Optical arbitrary waveform generation," Nat. Photonics **4**(11), 760–766 (2010).
5. G. B. Rieker, F. R. Giorgetta, W. C. Swann, J. Kofler, A. M. Zolot, L. C. Sinclair, E. Baumann, C. Cromer, G. Petron, C. Sweeney, P. P. Tans, I. Coddington, and N. R. Newbury, "Frequency-comb-based remote sensing of greenhouse gases over kilometer air paths," Optica **1**(5), 290–298 (2014).
6. T. J. Kippenberg, R. Holzwarth, and S. A. Diddams, "Microresonator-based optical frequency combs," Science **332**(6029), 555–559 (2011).
7. T. Herr, K. Hartinger, J. Riemensberger, C. Y. Wang, E. Gavartin, R. Holzwarth, M. L. Gorodetsky, and T. J. Kippenberg, "Universal formation dynamics and noise of Kerr frequency combs in microresonators," Nat. Photonics **6**(7), 480–487 (2012).
8. J. S. Levy, A. Gondarenko, M. A. Foster, A. C. Turner-Foster, A. L. Gaeta, and M. Lipson, "CMOS-compatible multiple-wavelength oscillator for on-chip optical interconnects," Nat. Photonics **4**(1), 37–40 (2010).
9. A. B. Matsko, A. A. Savchenkov, W. Liang, V. S. Ilchenko, D. Seidel, and L. Maleki, "Mode-locked Kerr frequency combs," Opt. Lett. **36**(15), 2845–2847 (2011).
10. S. A. S. Melo, A. R. do Nascimento, Jr., A. Cerqueira S, Jr., L. H. H. Carvalho, D. M. Pataca, J. C. R. F. Oliveira, and H. L. Fragnito, "Frequency comb expansion based on optical feedback, highly nonlinear and erbium-doped fibers," Opt. Commun. **312**, 287–291 (2014).
11. P. Klopp, U. Griebner, M. Zorn, and M. Weyers, "Pulse repetition rate up to 92 GHz or pulse duration shorter than 110 fs from a mode-locked semiconductor disk laser," Appl. Phys. Lett. **98**(7), 071103 (2011).
12. M. Hoffmann, O. D. Sieber, V. J. Wittwer, I. L. Krestnikov, D. A. Livshits, Y. Barbarin, T. Südmeyer, and U. Keller, "Femtosecond high-power quantum dot vertical external cavity surface emitting laser," Opt. Express **19**(9), 8108–8116 (2011).
13. H. Liu, J. Nees, and G. Mourou, "Diode-pumped Kerr-lens mode-locked Yb:KY$(WO_4)_2$ laser," Opt. Lett. **26**(21), 1723–1725 (2001).

#285271 https://doi.org/10.1364/OE.25.007627
Journal © 2017 Received 19 Jan 2017; revised 14 Mar 2017; accepted 21 Mar 2017; published 24 Mar 2017

Optics EXPRESS

14. W. Z. Zhuang, M. T. Chang, H. C. Liang, and Y. F. Chen, "High-power high-repetition-rate subpicosecond monolithic Yb:KGW laser with self-mode locking," Opt. Lett. **38**(14), 2596–2599 (2013).
15. A. A. Lagatsky, A. R. Sarmani, C. T. A. Brown, W. Sibbett, V. E. Kisel, A. G. Selivanov, I. A. Denisov, A. E. Troshin, K. V. Yumashev, N. V. Kuleshov, V. N. Matrosov, T. A. Matrosova, and M. I. Kupchenko, "Yb^{3+}-doped YVO_4 crystal for efficient Kerr-lens mode locking in solid-state lasers," Opt. Lett. **30**(23), 3234–3236 (2005).
16. G. Q. Xie, D. Y. Tang, L. M. Zhao, L. J. Qian, and K. Ueda, "High-power self-mode-locked Yb:Y_2O_3 ceramic laser," Opt. Lett. **32**(18), 2741–2743 (2007).
17. S. Uemura and K. Torizuka, "Kerr-lens mode-locked diode-pumped Yb:YAG laser with the transverse mode passively stabilized," Appl. Phys. Express **1**(1), 012007 (2008).
18. H. C. Liang, R. C. C. Chen, Y. J. Huang, K. W. Su, and Y. F. Chen, "Compact efficient multi-GHz Kerr-lens mode-locked diode-pumped Nd:YVO_4 laser," Opt. Express **16**(25), 21149–21154 (2008).
19. H. C. Liang, Y. J. Huang, W. C. Huang, K. W. Su, and Y. F. Chen, "High-power, diode-end-pumped, multigigahertz self-mode-locked Nd:YVO_4 laser at 1342 nm," Opt. Lett. **35**(1), 4–6 (2010).
20. Y. F. Chen, M. T. Chang, W. Z. Zhang, K. W. Su, K. F. Huang, and H. C. Liang, "Generation of sub-terahertz repetition rates from a monolithic self-mode-locked laser coupled with an external Fabry-Perot cavity," Laser Photonics Rev. **9**(1), 91–97 (2015).
21. Y. F. Chen, "Efficient 1521-nm Nd:$GdVO_4$ Raman laser," Opt. Lett. **29**(22), 2632–2634 (2004).
22. Y. F. Chen, "High-power diode-pumped actively Q-switched Nd:YVO_4 self-Raman laser: influence of dopant concentration," Opt. Lett. **29**(16), 1915–1917 (2004).
23. C. Y. Lee, C. C. Chang, H. C. Liang, and Y. F. Chen, "Frequency comb expansion in a monolithic self-mode-locked laser concurrent with stimulated Raman scattering," Laser Photonics Rev. **8**(5), 750–755 (2014).
24. V. N. Burakevich, V. A. Lisinetskii, A. S. Grabtchikov, A. A. Demidovich, V. A. Orlovich, and V. N. Matrosov, "Diode-pumped continuous-wave Nd:YVO_4 laser with self-frequency Raman conversion," Appl. Phys. B **86**(3), 511–514 (2007).
25. A. J. Lee, H. M. Pask, D. J. Spence, and J. A. Piper, "Efficient 5.3 W cw laser at 559 nm by intracavity frequency summation of fundamental and first-Stokes wavelengths in a self-Raman Nd:$GdVO_4$ laser," Opt. Lett. **35**(5), 682–684 (2010).
26. A. A. Demidovich, A. S. Grabtchikov, V. A. Lisinetskii, V. N. Burakevich, V. A. Orlovich, and W. Kiefer, "Continuous-wave Raman generation in a diode-pumped Nd^{3+}:$KGd(WO_4)_2$ laser," Opt. Lett. **30**(13), 1701–1703 (2005).
27. V. A. Lisinetskii, A. S. Grabtchikov, A. A. Demidovich, V. N. Burakevich, V. A. Orlovich, and A. N. Titov, "Nd:KGW/KGW crystal: efficient medium for continuous-wave intracavity Raman generation," Appl. Phys. B **88**(4), 499–501 (2007).
28. J. Jakutis-Neto, J. Lin, N. U. Wetter, and H. Pask, "Continuous-wave Watt-level Nd:YLF/KGW Raman laser operating at near-IR, yellow and lime-green wavelengths," Opt. Express **20**(9), 9841–9850 (2012).
29. D. C. Parrotta, W. Lubeigt, A. J. Kemp, D. Burns, M. D. Dawson, and J. E. Hastie, "Continuous-wave Raman laser pumped within a semiconductor disk laser cavity," Opt. Lett. **36**(7), 1083–1085 (2011).
30. M. T. Chang, W. Z. Zhuang, K. W. Su, Y. T. Yu, and Y. F. Chen, "Efficient continuous-wave self-Raman Yb:KGW laser with a shift of 89 cm^{-1}," Opt. Express **21**(21), 24590–24598 (2013).
31. C. Y. Tang, W. Z. Zhuang, K. W. Su, and Y. F. Chen, "Efficient continuous-wave self-Raman Nd:KGW laser with intracavity cascade emission based on shift of 89 cm^{-1}," IEEE J. Sel. Top. Quantum Electron. **21**, 1400206 (2015).
32. M. Kowalczyk, J. Sotor, and K. M. Abramski, "59 fs mode-locked Yb:KGW oscillator pumped by a single-mode laser diode," Laser Phys. Lett. **13**(3), 035801 (2016).
33. H. Zhao and A. Major, "Powerful 67 fs Kerr-lens mode-locked prismless Yb:KGW oscillator," Opt. Express **21**(26), 31846–31851 (2013).
34. B. Metzger, A. Steinmann, F. Hoos, S. Pricking, and H. Giessen, "Compact laser source for high-power white-light and widely tunable sub 65 fs laser pulses," Opt. Lett. **35**(23), 3961–3963 (2010).
35. H. Zhao and A. Major, "Megawatt peak power level sub-100 fs Yb:KGW oscillators," Opt. Express **22**(25), 30425–30431 (2014).
36. D. J. Spence, P. Dekker, and H. M. Pask, "Modeling of continuous wave intracavity Raman lasers," IEEE J. Sel. Top. Quantum Electron. **13**(3), 756–763 (2007).

1. Introduction

Optical frequency combs (OFCs) are optical coherent sources formed by a series of regularly spaced spectral lines. They are very attractive in a variety of research fields including fundamental physics, spectroscopy, time-frequency metrology, terahertz (THz) generation, optical communications, and microwave photonics [1–5]. Up to now, the promising approaches comprise the four-wave mixing in micro-cavities [6–9] and the mode locking in laser resonators [10–12]. The former method can generate extremely wide OFCs with high repetition rates, but requires a cavity with physical size to fix the line spacing and a set-up

Optics EXPRESS

with several stages. On the other hand, although passively mode-locked (ML) lasers or fiber lasers are often used to generate high quality frequency combs, the high-repetition-rate ML systems usually involve great complexity of cavity designs. Therefore, it is greatly desirable to develop compact ML laser systems with the reduction of complexity and the enhancement of stability. Compact ML lasers with wide frequency spans and high repetition rates would expand the range of applications even further.

The self-mode-locking (SML) without using active elements or saturable absorbers is a feasible way to achieve compact ML lasers. The advent of diode-pumped laser technology and fast real-time detection systems have opened up a number of new developments on the SML operation [13–20]. In addition to the Kerr lens effect, the mechanism for the SML in short linear cavities is mainly attributed to the large mode spacing to prevent the mode competition [14, 20]. The SML pulse train with the repetition rate of several tens of GHz was successfully demonstrated in the monolithic Yb:KGW crystal laser [14]. With the ML monolithic laser, a coupled cavity scheme was further used to multiply the repetition rate up to sub-THz [20].

One noteworthy discovery is that the laser crystals used to achieve the SML operation can also be exploited to be the Raman gain media due to their intense Raman modes. Consequently, these laser crystals can be employed to generate the so-called self-Raman frequency conversion via stimulated Raman scattering (SRS) [21–25]. Figure 1(a) shows the spontaneous Raman spectrum of KGW crystal (Micro Raman Identify / ProTrusTech Co., Ltd), in which two strong Raman modes at 901 and 768 cm^{-1} are often used to obtain the Stokes wave with large frequency shifts [26–28]. In addition to these two Raman modes, the self-Raman laser at the lowest frequency mode near 89 cm^{-1} has been successfully demonstrated in recent years [29–31]. This progress provokes an intriguing prospect whether the frequency spectra generated by the SML and SRS process can be linked together to expand the OFC significantly.

In this work we numerically analyze and experimentally accomplish the broad expansion the OFC by the self-Raman scattering in a coupled-cavity SML monolithic Yb:KGW laser. We firstly design a coated Yb:KGW crystal to generate the OFC in the SML operation. The crystal length shorter than 3.00 mm is used to avoid significant re-absorption losses. With a crystal length of 2.93 mm, the SML repetition rate of 25.78 GHz is obtained. We then employ a partially reflective mirror to form a coupled cavity that was set to multiply the repetition rate to reach 128.9 GHz. Furthermore, the critical value of the coupled reflectivity for the generation of self-Raman scattering is systematically explored and found to be approximately 90%. Experimental results reveal that a coupled reflectivity of 95% can lead to the generation of the first- and second-order SRS in the gain medium at the lowest frequency mode. As a result, the OFC can be expanded up to 8.4 THz with the pulse width down to 53 fs. The total output power for the fundamental and the Stokes waves can achieve 1.6 W at a pump power of 8.7 W. Previously, several groups demonstrated sub-100 fs Yb:KGW mode-locked lasers with the action of a semiconductor saturable absorber mirror (SESAM) or Kerr-lens [32–35]. The repetition rates in these earlier works were in the range of 30-80 MHz, whereas the present method can generate the repetition rate greater than 100 GHz. Our exploration confirms that the optical spectra generated by the SML and SRS process can be linked together to obtain an ultrahigh-repetition-rate broadband OFC.

2. Laser configuration and design principles

Figure 1(b) shows the laser configuration that consists of a monolithic crystal to generate the self-mode-locked pulse train and an external reflective mirror to multiply the repetition rate. To manifest the optical spectrum realistically, the frequency distribution of the self-mode-locked emission is expressed by an analytical form based on the damped harmonic oscillator as

Optics EXPRESS

$$I_o(v)=\sum_{n=-N}^{N}\frac{A_n\,\gamma v^2}{[v^2-(v_o+n v_{ML})^2]^2+(\gamma v)^2}, \tag{1}$$

where A_n is the weighting coefficient, γ is the effective linewidth of the lasing mode, v_o is the central frequency, $v_{ML}=c/2L^*_{cry}$ is the mode spacing of the monolithic cavity, c is the speed of light in vacuum, $L^*_{cry}=n_r L_{cry}$, n_r is the refractive index of the gain medium, and L_{cry} is the geometric length of the gain medium. From Eq. (1), the effective bandwidth of the mode-locked comb can be found to be $(2N+1)\,v_{ML}$. The spectrum $I_o(v)$ in Eq. (1) is used to express the overall profile in the gain medium.

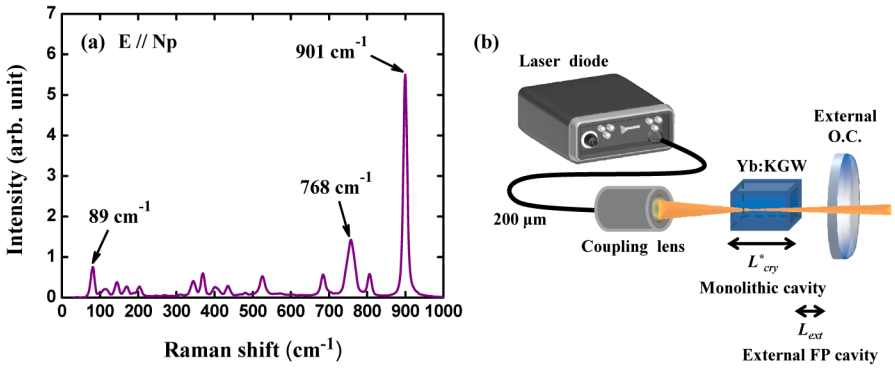

Fig. 1. (a) Spontaneous Raman spectrum of $KGd(WO_4)_2$ for the N_p polarization scattering geometry. (b) Experimental setup for a diode-pumped Yb:KGW couple-cavity laser with harmonically SML and SRS concurrently.

The spectral transmission function of an external FP filter with the length of L_{ext} is given by [21]

$$T_{FP}(v)=\frac{(1-R_o)(1-R_e)}{\left(1-\sqrt{R_oR_e}\right)^2+4\sqrt{R_oR_e}\left[\sin\left(\frac{\pi v}{v_{ML}}\frac{L_{ext}}{L^*_{cry}}\right)\right]^2}, \tag{2}$$

where R_o is the reflectivity of the output surface of the laser crystal and R_e is the reflectivity of the external FP mirror. The frequency spectrum for the self-mode-locked pulses passing through the external FP cavity can be expressed as

$$I_F(v)=\frac{(1-R_o)(1-R_e)}{\left(1-\sqrt{R_oR_e}\right)^2+4\sqrt{R_oR_e}\left[\sin\left(\frac{\pi v}{v_{ML}}\frac{L_{ext}}{L^*_{cry}}\right)\right]^2}\sum_{n=-N}^{N}\frac{A_n\,\gamma v^2}{[v^2-(v_o+n v_{ML})^2]^2+(\gamma v)^2}. \tag{3}$$

The numerical calculation with Eq. (3) can reveal that when the cavity ratio L_{ext}/L^*_{cry} is set to a rational number q/p, the mode spacing in the coupled cavity spectrum $I_F(v)$ turns into the pth order harmonics of the mode spacing of the monolithic cavity, i.e. pv_{ML}. The frequency multiplication with the coupled FP cavity has been experimentally confirmed.

The Yb:KGW crystal is possible to simultaneously act as a Raman gain medium to attain the self-Raman laser action, as long as the intracavity power of the fundamental wave exceeds

Optics EXPRESS

the threshold of the SRS process. The diode pump power required to reach the Raman threshold is given by [36]

$$P_P = \frac{A_S}{g_R L_{cry}} \frac{\lambda_F}{\lambda_P} \frac{(T_S + \gamma_S)(T_F + \gamma_F)}{2}, \tag{4}$$

where A_S is the spot area of the Stokes field, g_R is the stimulated Raman gain coefficient, λ_P is the wavelength of the pump radiation, λ_F is the wavelength of the fundamental wave, T_F, γ_F and T_S, γ_S are the output coupling transmissions and round-trip losses for the fundamental and Stokes fields, respectively. The stimulated Raman gain coefficient for a Raman crystal pumped by a fundamental wave with a narrow laser line v_F is given by [27]

$$g_R = \frac{8\pi c^2 N_o}{\hbar n_s^2 v_S^2 \Gamma} \left(\frac{\partial \sigma}{\partial \Omega} \right), \tag{5}$$

where $v_S = v_F - v_R$ is the frequency of the Stokes wave, v_R is the frequency of the Raman shift, Γ is the linewidth of the Raman transition (half-width at half-maximum), $\partial\sigma / \partial\Omega$ is the integrated scattering cross section, N_o is the number of Raman-active molecules, and n_s is the refractive index of the Raman media for the Stokes frequency. For the present coupled cavity, the output transmission for the fundamental wave with the minimum transmission is given by $T_F = (1 - R_o)(1 - R_e)$. Note that the fundamental wave with the minimum transmission can lead to the lowest threshold for lasing. If the lasing bandwidth of the mode-locked fundamental wave $I_F(v)$ can be wider than the frequency shift of the Raman mode, the frequency combs of the fundamental and Stokes waves are possible to be closely linked together with any gap. In this work, the lowest Raman frequency shift involving the 89 cm^{-1} mode is considered to explore the linkage of OFCs generated by the SML and SRS processes in the Yb:KGW crystal. Since the optical bandwidths of the resonator coatings can be designed to be wider than the frequency shift by the 89 cm^{-1} Ramon mode, the output transmissions for the fundamental and Stokes waves are regarded to be nearly the same, i.e. $T_S \approx T_F$. From Eq. (4), the SRS threshold for the 89 cm^{-1} Raman mode is estimated to be down to 2.5 W as long as the coupled laser cavity with $L_{cry} = 3$ mm is maintained at the quality of $T_F = T_S = 0.1\%$ and $\gamma_F = \gamma_S = 0.05\%$. Note that the orders of $T_F = T_S = 0.1\%$ and $\gamma_F = \gamma_S = 0.05\%$ are the values that can be realistically achieved in experiment.

Assuming the wavelength conversion to be generally homogeneous for each lasing mode, the frequency spectrum for the mode-locked oscillation with the multiorder Stokes emissions can be given by

$$I_T(v) = \left(1 - \sum_{m=1}^{M} \eta_m\right) I_F(v) + \sum_{m=1}^{M} \eta_m I_F(v + m v_R), \tag{6}$$

where η_m is the conversion efficiency for the mth order Stokes emission. Specifically, if $(2N+1) v_{ML} > v_R$, the whole frequency comb in Eq. (6) can be widely spread without any gap. Figure 2 illustrates the example of the mode-locked frequency comb in the Yb:KGW laser expanded by the first and second orders SRS process on the 89 cm^{-1} line with the parameters of $v_{ML} = 25.78$ GHz, $L_{ext} / L_{cry}^{*} = 1/5$, $A_n = e^{-n^2/2\sigma^2}$, $\sigma = 25$, $N = 75$, $\gamma = 10$ kHz, $v_R = 2.67$ THz, $\eta_1 = 0.33$, and $\eta_2 = 0.33$. The parameter values used in the calculation are associated with the following experiment.

Optics EXPRESS

3. Experimental results and discussion

The gain medium was a 5.0-at.% doped Yb:KGW crystal and cut along the n_g-axis. To avoid significant re-absorption losses, the crystal length was chosen to be shorter than 3.00 mm. Here the precise length is 2.93 mm. The laser crystal was coated to be the monolithic cavity that could achieve the self-mode-locked operation [14]. The first facet of the crystal was coated for high reflection (R>99.8%) in the range of 1030 nm and 1130 nm and high-transmission (T>95%) at 980 nm to serve as the front mirror. The second facet was coated for high reflection (R>99%) at 980 nm to increase the absorption efficiency of the pump power and was coated for partial reflection (R≈98%) in the range of 1030 nm and 1130 nm to form the output coupler. The Yb:KGW crystal was wrapped with indium foil and mounted within a water-cooled copper heat sink. The water temperature was set at 8°C to prevent the laser crystal from condensation. The pumping source was a 10-W 980-nm fiber-coupled laser diode with a core diameter of 200 μm and a numerical aperture of 0.2. A lens with a focal length of 25 mm was used to focus the pump beam into the laser crystal. The pump spot radius was approximately 110 μm.

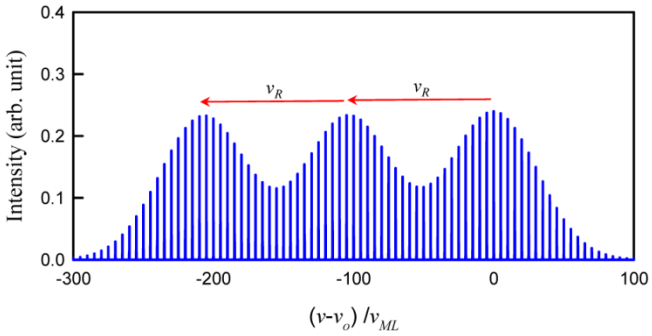

Fig. 2. Numerical example of the mode-locked frequency comb in the Yb:KGW laser expanded by the first and second orders SRS process on the 89 cm^{-1} line.

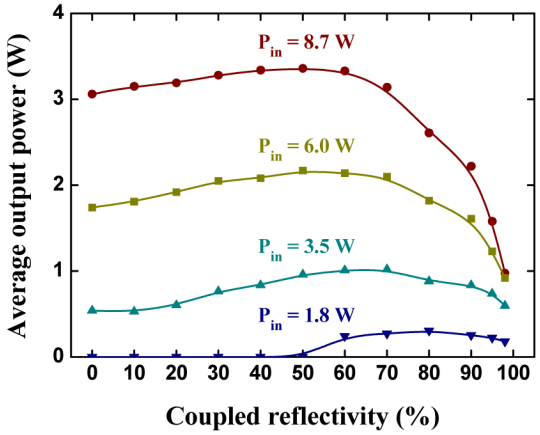

Fig. 3. (a) The average output power versus the coupled reflectivity for several incident pump powers in the scheme of the coupled cavity.

A flat wedged mirror with partial reflection covering the lasing bandwidth was closely behind the monolithic laser to constitute the external FP cavity. Several different reflection values for the flat mirror were used to explore the influence of the coupled cavity on the output power and lasing spectrum. Figure 3 shows the average output power versus the reflectivity of the flat mirror for several incident pump powers in the scheme of the coupled

Optics EXPRESS

cavity. Since the average output power is nearly the same for the ratio L_{ext}/L^*_{cry} in the range of 0.0–1.0, hereafter all experimental results for the case of $L_{ext}/L^*_{cry}=1/5$ are shown for convenience, unless otherwise specified. Note that the roundtrip cavity excess losses increases with increasing the coupled cavity length. On the other hand, the higher order the harmonic mode locking, the more sensitive the coupled cavity length. By making a compromise with these two factors, the coupled cavity length of $L_{ext}/L^*_{cry}=1/5$ was adopted. It can be seen that there is an optimal reflectivity R_e for the coupled mirror to achieve the maximal output power for a given pump power. In general, the output power decreases considerably for the coupled mirror with $R_e \geq 90\%$ for far above the lasing threshold. Nevertheless, as shown in the following the lasing optical spectrum was found to reveal the generation of the SRS on the 89 cm^{-1} line for $R_e \geq 90\%$.

The lasing optical spectrum was measured by using a Michelson interferometer (Advantest Q8347) with Fourier transform to reach the resolution as high as 0.003nm. Figure 4(a) shows the lasing spectrum for the SML operation without the coupled cavity and Figs. 4(b)-4(e) show the lasing spectra with the coupled cavity with R_e = 50%, 60%, 70%, and 80%, respectively, at the pump power of 8.7 W. As shown in Fig. 4(a), the lasing bandwidth Δv_B is approximately $30v_{ML}$ for the operation without the coupled cavity, where $v_{ML}=25.78$ GHz. It can be seen that the coupled cavity not only increases the lasing bandwidth up to the range of $100v_{ML}$ but also changes the mode spacing to be approximately $5v_{ML}=128.9$ GHz which is consistent with the theoretical analysis for $L_{ext}/L^*_{cry}=1/5$.

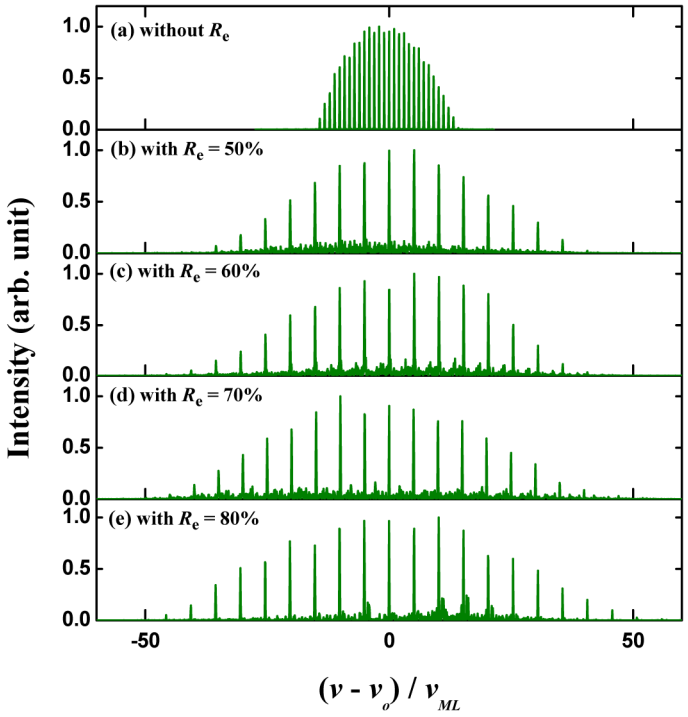

Fig. 4. Lasing spectra for the SML operation (a) without the coupled cavity; (b) with R_e = 50%; (c) 60% ; (d) 70%; and (e) 80% at the pump power of 8.7 W.

From Figs. 3 and 4, it can be found that the intensity levels of the output pulse trains with R_e = 50-70% are higher than those with R_e = 80-95%. Even so, the intracavity intensity level

Optics EXPRESS

generally increases with increasing the value of R_e. In the intracavity SRS process, the higher the intracavity intensity level, the lower the SRS threshold. Experimental results clearly reveal that the SRS process can be generated for the coupled cavity mirror with R_e>90%. By making a compromise with the output efficiency, the optimal performance for expanding the OFC can be obtained with R_e = 95%. Figure 5 shows the lasing optical spectrum versus the pump power for the coupled cavity with R_e = 95%. It can be seen that the first-order Stokes wave starts to appear at the pump power of 2.6 W. Increasing the pump power to 6.0 W, not only the first-order but also the second-order Stokes waves are simultaneously generated. As seen in Fig. 5, the uniformity of the frequency peaks is better at the pump power of 6.0-6.9 W than that at higher pump power. Even so, the lasing bandwidth of the optical spectrum can reach the maximum value of approximately 8.4 THz at the pump power around 8.7 W. In other words, the optimal pump power for the best uniformity is slightly lower than that for the widest bandwidth. It is worth noting that the second-order Stokes wave will dominate the output emission for the pump power higher than 9.5 W. In other words, there is an optimal pump power for achieving the output balance between the fundamental and first- and second-order Stokes waves. In the present case, the optimal pump power is approximately 8.7 W, at which the total output power can be maintained at 1.6 W.

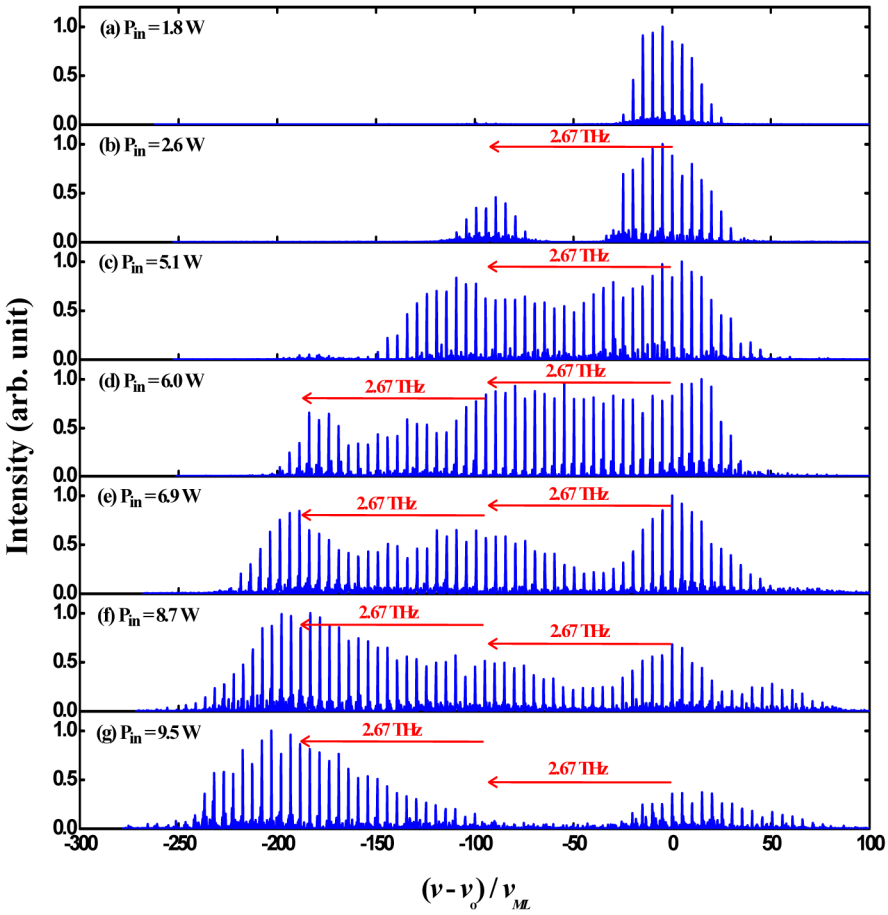

Fig. 5. The lasing optical spectrum versus the pump power for the coupled cavity with R_e = 95%.

Figure 6 show a comparison between the numerical analysis and experimental spectrum for the case at the pump power of 8.7W. The experimental and numerical results are

Optics EXPRESS

displayed as mirror images. The parameters used in the calculation are $v_{ML} = 25.78\,\text{GHz}$, $L_{ext} / L^{*}_{cry} = 1/5$, $A_n = e^{-n^2/2\sigma^2}$, $\sigma = 25$, $N = 75$, $\gamma = 10\,\text{kHz}$, $v_R = 2.67\,\text{THz}$, $\eta_1 = 0.26$, and $\eta_2 = 0.39$. It can be seen that the experimental spectrum agrees very well with the numerical analysis. Since the pulse repetition rate was beyond the sampling rate of the contemporary oscilloscope, the methods of first- and second-order autocorrelations were used to acquire the temporal behavior of the laser output. The first-order autocorrelation trace was measured with a Michelson interferometer (Advantest Q8347). The second-order autocorrelation trace was measured with a commercial autocorrelator (APE pulse check, Angewandte Physik & Elektronik GmbH). Figure 7(a) shows the experimental result of the first-order autocorrelation obtained at the average output power of 1.6 W for the coupled cavity with R_e = 95%. The characteristic of the temporal trace can be clearly seen to be equivalent to the harmonically mode-locked oscillation with the fifth order harmonics of the mode spacing of the monolithic cavity, i.e. $5v_{ML} = 128.9$ GHz. The full width at half maximum of the single pulse of the second-order autocorrelation trace is shown in Fig. 7(b). Assuming the Gaussian shaped temporal profile, the pulse duration is estimated to be 53 fs. Consequently, the time bandwidth product of the mode-locked pulse is found to be 0.445, which is rather close to the Fourier-limited value of 0.441.

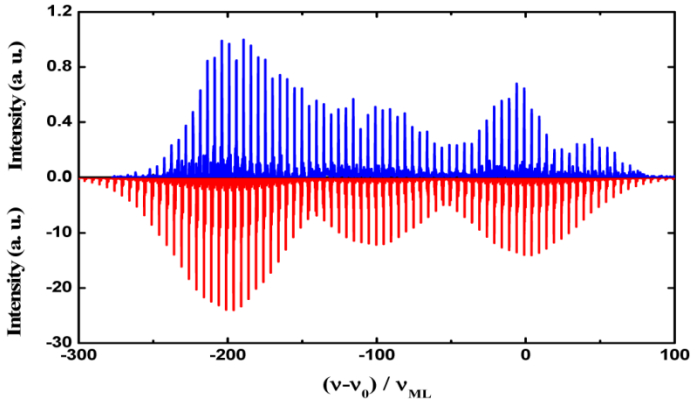

Fig. 6. A comparison between the numerical analysis and experimental spectrum for the case at the pump power of 8.7W. The experimental and numerical results are displayed as mirror images.

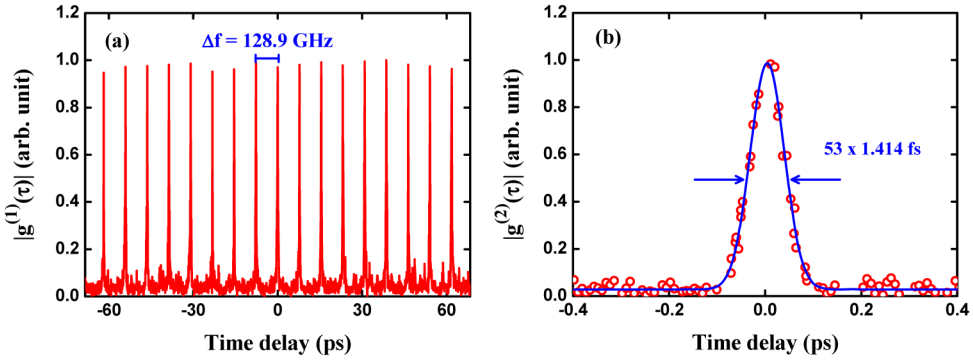

Fig. 7. (a) Experimental result of the first-order autocorrelation obtained at the average output power of 1.6 W for the coupled cavity with R_e = 95%. (b) The full width at half maximum of the single pulse of the second-order autocorrelation trace.

Optics EXPRESS

1. Conclusion

In summary, we have developed a promising approach to broadly expand the OFC by the self-Raman scattering at the lowest frequency mode in a coupled-cavity SML monolithic Yb:KGW laser. The experiment was accomplished by using a coated Yb:KGW crystal to achieve the monolithic SML operation and using a partially reflective mirror to enhance the intracavity power for generating the self-Raman process. The length of the coupled cavity was set to multiply the repetition rate up to 128.9 GHz. Experimental results reveal that a coupled reflectivity of 95% can lead to the generation of the first- and second-order SRS in the gain medium at the lowest frequency mode. The OFC was consequently expanded to reach approximately 8.4 THz with the pulse width down to 53 fs. At a pump power of 8.7 W, the total output power for the fundamental and the Stokes waves can achieve 1.6 W. The present result is believed to offer a useful method for generating the ultrahigh-repetition-rate broadband OFC via the simultaneous SML and SRS processes.

Funding

This work is supported by the Ministry of Science and Technology, Taiwan (Contract No. MOST 105-2628-M-009-004).